- Technical Paper -

CHLORIDE-INDUCED CORROSION PRODUCTS OF STEEL BARS IN CONCRETE

LI Xuezhong[*1], WU Qing [*2] and LI Zhuguo[*3]

ABSTRACT

In this paper, the intermediate products, including aka-ganeite (β–FeOOH) and lepidocrocite (γ–FeOOH), and the final products, including hematite (α–Fe_2O_3), maghemite (γ–Fe_2O_3) and goethite (α–FeOOH), of steel corrosion in seawater & sea sand-based concrete under different environments were investigated by the XRD and SEM. In the seawater immersion-dry repeating environment, the α–FeOOH, α–Fe_2O_3 and magnetite (Fe_3O_4) converted mutually. Also, in the seawater environment, the γ–FeOOH and β–FeOOH substituted for oxygen as the new depolarizers of cathode reduction reaction.

Keywords: concrete, seawater, sea sand, corrosion, XRD, SEM

1. INTRODUCTION

Chloride ions contained in concrete pose a great threat to steel bars by destroying integrality of the steel bars' passive film to result in corrosion of the steel bars and a significant reduction of service life of concrete structure [1-2].

Many researchers have extensively studied the corrosion of steel bars in concrete caused by chloride ions, Refait et al. [3] found that, in the presence of chloride ions, ferrous hydroxide reacts with chloride first to produce a very unstable green rust hydrochloride $GRCl^{-}([Fe_3^{2+}Fe^{3+}(OH^{-})_8]^{+}\cdot[Cl^{-}\cdot nH_2O]^{-}$ containing ferrous and ferric iron, and then it continues to oxidize into β–FeOOH or γ–FeOOH as an intermediate transition product. Legrand et al. [4] established that, in the presence of SO_4^{2-}, ferrous hydroxide reacts with sulfate to form green rust sulfate $GRSO_4^{2-}([Fe_4^{2+}Fe_2^{3+}(OH^{-})_{12}]^{2+}\cdot[SO_4^{2-}\cdot 2H_2O]^{2-})$ first, and then continues to oxidize to γ–FeOOH as an intermediate transition product. At the initial stage of corrosion, the products are mainly γ–FeOOH.

Although there are many studies on the effect of chloride ion on steel bars, these studies remained at macro-mechanical properties. The studies on phase composition and micro-structure of rust layer in concrete are still lacking in systematic theory, which cannot accurately describe the mechanism of steel corrosion in concrete having high concentration of chloride.

In view of the main problems of coastal concrete durability at present, concrete specimens, using seawater and sea sand, were prepared in this study to simulate the corrosion of steel bar continuously immersion in the marine environment, and marine environment with dry-wet cycling respectively. SEM was used to photograph and analyze on the surface of steel bars, and the compound type, generation time and the effect of corrosion products on steel bar matrix were discussed based on the morphology. X-ray diffraction was used to obtain the diffraction patterns of corrosion products gathered from different rust layers of steel bar, and the composition and internal structure of the products were investigated. The main intermediate products, including lepidocrocite (γ–FeOOH) and aka-ganeite (β–FeOOH), and the final oxidation products, including maghemite (γ–Fe_2O_3), hematite (α–Fe_2O_3) goethite (α–FeOOH), of steel corrosion in the concrete converted mutually under different environments. Also, the mutual transformation between the intermediate and final corrosion products was clarified.

2. EXPERIMENTAL PROGRAM

2.1 Preparation of Specimens

Cylindrical specimens with dimensions of Φ×L=52mm×320mm were prepared to ensure that the corrosion of the embedded steel bar in all directions was identical. The cement used was ordinary Portland cement. Seawater was used. Unwashed sea stone and sea sand were used as aggregates. The fine modulus F.M. of sea sand was 2.65 and the chloride ion content was 0.24%. The mix proportions of the concrete were as cement: water: sand: stone= 1: 0.41: 1.05: 2.58 by mass.

All the steel bars embedded in the concrete specimens came from the same batch of low carbon steel, which were hot rolled plain bars 235 (China National Standards) with a diameter of 12 mm. The non-iron elements of the steel bars are shown in Table 1. Each steel bar was 320 (±1) mm in length. Two bare ends of each steel bar were coated with anti-rust paint to ensure

Table 1. Composition of steel (%)

Element	C	Si	Mn	P	S
content (%)	0.16	0.24	0.46	0.032	0.029

*1 Graduate Student, Graduate School of Sci. and Tech. for Innovation, Yamaguchi University, JCI Member
*2 College of Civil Engineering and Architecture, Jiangsu University of Science and Technology
*3 Prof., Graduate School of Sci. and Tech. for Innovation, Yamaguchi University, Dr.Eng., JCI Member

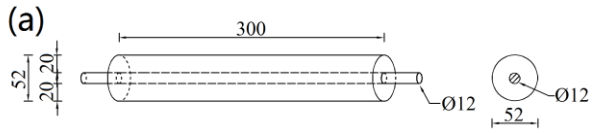

Fig.1 Details of test specimen;
(a) Dimension, (b) Photograph

them non-corrosion. The dimensions and photograph of the specimens are shown in Fig.1.

2.2 Accelerated Corrosion of Steel Bar

After the specimens were made, they were placed in a curing room in two groups. One group was immersed continuously in artificial seawater with 1.48% concentration of Cl^- to simulate sea environment [5]. Another group was exposed to the seawater-dry repeating to simulate the environment sea humidity change, where the specimens were immersed in the artificial seawater for two days and then dried for two days. The water temperature was 20±5℃ (Fig.2). The grouping of specimens is shown in Table 2.

2.3 XRD Analysis

Firstly, the corroded steel bars were taken out from concrete. The corrosion layers were divided into internal rust layer and external rust layer according to their structures. The external rust layer was loose and could be easily exfoliated. The internal rust layer with compact structure was closely connected with the reinforced bar matrix. Two kinds of rust powder were grinded separately in grinding bowls until they passed through 330 mesh sieves. The test process was as 1) placed the rust powder (about 2g) on the supporting slide, 2) smoothed the surface, and 3) placed the sample into the X-ray powder diffractometer shown in Fig.3 (XRD-6000, Shimadzu Company, Japan). After the XRD analysis, the test results were output from the computer

Table 2. Test specimen grouping

Specimen Name	Accelerated Corrosion Method	Exposure Period	
A1	Only seawater immersion	2 months	6 months
A2	Seawater immersion-drying repeating	2 months	6 months

Fig.2 Accelerated corrosion test; (a) Immersion, (b) Wet/dry cycles

Fig.3 XRD-6000 model X-ray powder diffractometer

and analyzed by software MDI Jade 6.5.

2.4 SEM Analysis

After the concrete specimens were roughly broken, they were hammered into soybean-sized

Fig.4 Nova NanoSEM450 scanning electron microscope (SEM)

particles. Then, one or two pieces of cement paste flake were gathered from the surface of steel bars with corrosion products. The paste specimens were packed in sealed bags under vacuum to prevent the corrosion products from continuing to oxidize in the air. The prepared samples were analyzed by Nova NanoSEM450 field emission scanning electron microscope (see Fig.4). Corrosion products were observed three times at the same location. The magnifications were 2000 and 10000 times respectively.

3. RESULTS AND DISCUSSION

3.1 Products of steel rust layer

X-ray diffraction spectra of powder samples of the inner rust layer and the outer rust layer of steels are shown in Fig.5. It can be seen from graphs that the corrosion products of steel were a mixture of wustite (FeO), aka-ganeite (β–FeOOH), lepidocrocite (γ–FeOOH), goethite (α–FeOOH), magnetite (Fe_3O_4), maghemite (γ–Fe_2O_3), and hematite (α–Fe_2O_3). Among them, the diffraction peaks of maghemite (γ–Fe_2O_3), hematite (α–Fe_2O_3), lepidocrocite (γ–FeOOH), and goethite (α–FeOOH) were higher, indicating that there were many rust products, or their crystallinity was higher. In addition, some cement hydration products such as orthoclase, calcium silicate hydrate, calcium aluminate hydrate and iron were also present in the samples, possibly due to the mutual infiltration of rust products and the hydrates.

From Fig.5, it can be seen that the outer rust layer of steel bars was mainly composed of wustite (FeO), magnetite (Fe_3O_4), goethite (α–FeOOH) and maghemite (γ–Fe_2O_3), while the inner rust layer was mainly composed of a mixture of goethite (α–FeOOH), magnetite (Fe_3O_4), aka-ganeite (β–FeOOH), hematite (α–Fe_2O_3) and lepidocrocite (γ–FeOOH). Also, for the same sample treatment, quality and environments, the diffraction peak intensity of the goethite (α–FeOOH) of the outer rust layer was higher, because the outer rust layer contacted directly with the moisture with chloride. Due to the lack of oxygen, there is more magnetite (Fe_3O_4) and lepidocrocite (γ–FeOOH) in the inner rust layer. The structural model of steel bar corrosion caused by chloride is shown in Fig.6.

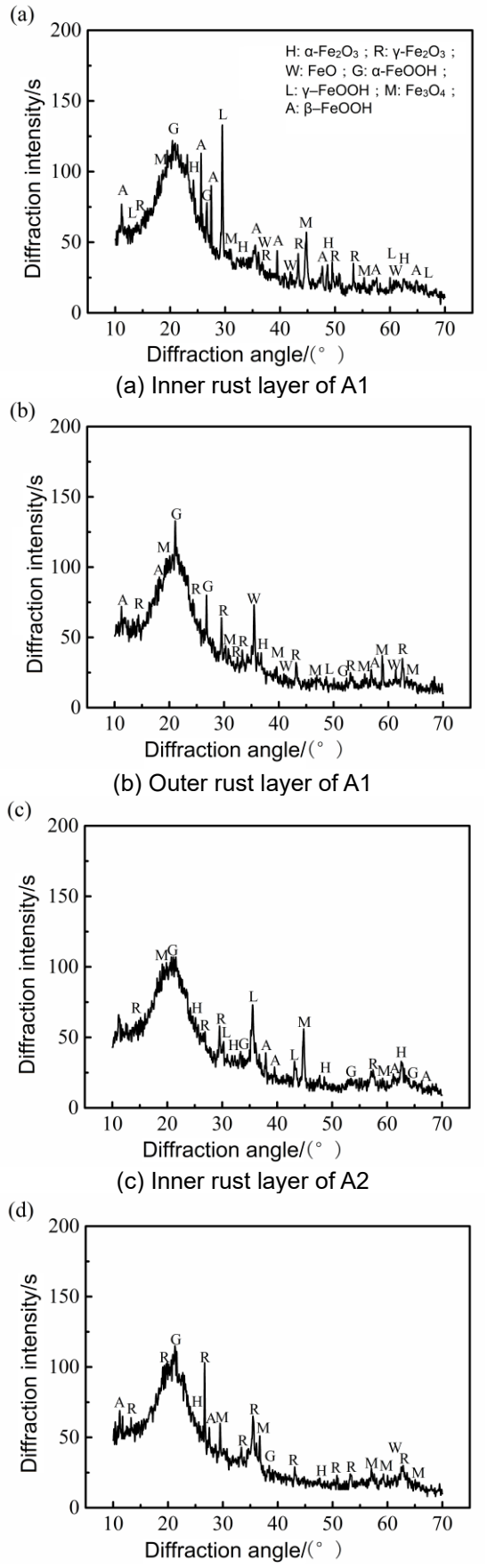

(a) Inner rust layer of A1

(b) Outer rust layer of A1

(c) Inner rust layer of A2

(d) Outer rust layer of A2

Fig.5 XRD charts of rust samples of steel bars

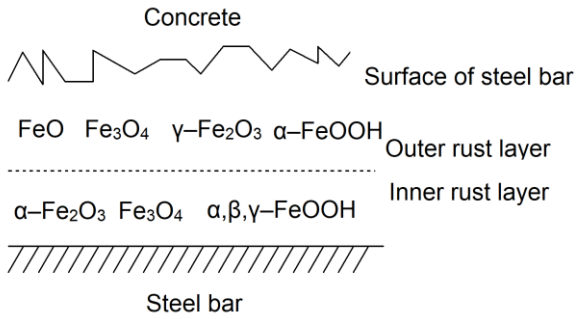

Fig.6 Corrosion layer structure of rusted rebar

Misawa [6] reported that lepidocrocite (γ–FeOOH) and goethite (α–FeOOH) are denser than aka-ganeite (β–FeOOH) with monoclinic cell structure. Moreover, because Cl^- and OH^- can stablize the pores, water can be retained in the gap between aka-ganeite (β–FeOOH) acicular crystals, providing favorable conditions for carbon steel to aggravate pitting corrosion. Also, Cl^- can replace the OH^- radical of aka-ganeite (β–FeOOH) and form a new corrosion product phase β–FeO(OH,Cl).

Previous studies [7] have found that some components of corrosion products of steel bar can act as new depolarizers in cathodic reduction reaction without oxygen. This explains why the corrosion of steel bar can continue for a long term in concrete specimens even there's no oxygen. When the sample A1 was immersed in seawater for a long time, though oxygen supply was limited, the substitution in the rust layer of carbon steel became a new depolarizer. Thus, cathodic reduction reaction occurred at the interface where the resulting corrosion could be described by the following equation [8]:

$$6FeOOH + 2e^- \rightarrow 2Fe_3O_4 + 2H_2O + 2OH^- \quad (1)$$

The above chemical reaction not only solves the stagnation of cathodic reduction reaction caused by lack of oxygen, but also reduces the resistance of hydrates in the transmission process with the dissolution of FeOOH attached to the steel matrix. It can be concluded that the solution layer near the surface of steel bar contained high concentration of Fe^{2+}. Without the barrier of FeOOH, the anodic iron dissolved rapidly and the anodic polarization of carbon steel decreased rapidly. With the progress of corrosion process, FeOOH, as a cathode depolarizer under anoxic condition, was gradually depleted. At this time, a large number of Fe_2O_3 and Fe_3O_4 corrosion products were accumulated on the surface of steel bar.

3.2 Microstructure of steel rust layer

In order to understand the morphological characteristics of the corrosion layer, the morphology of the corroded layer was observed by SEM. Fig.7 and Fig.8 are the SEM images of the morphology of corrosion products of carbon steel after 2 month and 6 months. It can be seen that the corrosion products exhibited different morphologies, such as rod, needle, scale, granular, and block. The corrosion products were integrated with the cross-network attached to the surface of steel bar. Based on the XRD results, it can be inferred that the large-sized products were magnetite (Fe_3O_4), needle-like or rod-like products were goethite (α–FeOOH), the cross-network of corrosion products was aggregates of lepidocrocite (γ–FeOOH) and goethite (α–FeOOH), while the spherical, scaly and granular products were a mixture of hematite (α–Fe_2O_3) and maghemite (γ–Fe_2O_3). α–FeOOH can adhere to the surface of steel bar, so the dissolution rate of anodic iron decreases. This is the main reason why the corrosion rate of steel bar decreased gradually with the progress of corrosion. According to the elemental compositions determined by EDS (see Table 3), the corrosion products included not only iron oxides, but also cement hydration products such as orthoclase, calcium silicate hydrate and calcium aluminate hydrate. This was likely due to the infiltration of corrosion products into cement paste.

Table 3. Elemental compositions of powder measured by EDS (%)

Specimen Name	O	Si	Ca	Fe
A1	51.16	2.42	3.75	42.66
A2	35.12	1.32	4.82	58.74

From Fig.7, it can be seen that the corrosion products of steel bars in chloride environment exhibited massive and granular morphology at 2 months and 6 months, but the structure was relatively loose. Combined with the XRD results, it can be inferred that the corrosion product was mainly composed of goethite (α–FeOOH), magnetite (Fe_3O_4) and lepidocrocite (γ–FeOOH). The goethite (α–FeOOH) was the major component and was formed by the reaction of rust intermediates of steel bar immersed in the seawater.

Due to the long-term immersion of the specimens, it was difficult for oxygen to reach the surface of steel bars during the corrosion process. Thus, the other part of the specimens was oxidized incompletely and became black magnetite (Fe_3O_4).

Fig.8 shows the SEM morphology of 2 months and 6 months products of carbon steel in concrete specimens under dry-wet cycling. It can be seen from the images that the corrosion products at 2 months were mostly granular aggregates with compact texture, including some acicular and flaky products, which are typical maghemite (γ–Fe_2O_3). Combined with the XRD results, it was inferred that the content of magnetite (Fe_3O_4) and maghemite (γ–Fe_2O_3) was higher in the corrosion product. According to Legrand's theory, due to a large amount of sulfate contained by the seawater, it reacts with $Fe(OH)_2$ to firstly produce green rust hydrochloride $GRCl^-$ ($[Fe_3^{2+}Fe^+(OH^-)_8]^+ \cdot [Cl^- \cdot nH_2O]^-$), and then green rust hydrochloride $GRCl^-$ ($[Fe_3^{2+}Fe^+(OH^-)_8]^+ \cdot [Cl^- \cdot nH_2O]^-$) continues to oxidize to produce orange-yellow lepidocrocite (γ–FeOOH). At the same time, the labile $Fe(OH)_2$ was transformed into the wustite (FeO) partially. Due to the moisture with chloride, lepidocrocite (γ–FeOOH) was transformed into magnetite (Fe_3O_4), and magnetite (Fe_3O_4) finally formed maghemite (γ–Fe_2O_3) through secondary changes under sufficient oxygen conditions. The related reaction

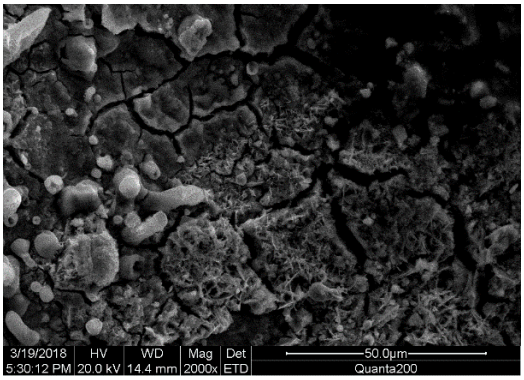

(a) 2 months rust layer morphology of A1 (x2000)

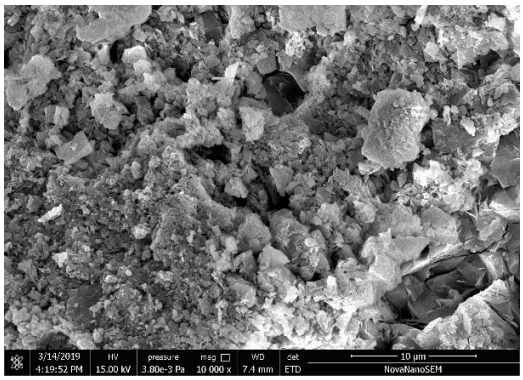

(b) 6 months rust layer morphology of A1 (x10000)

Fig.7 SEM images of rust layer of steel bar immersed in the seawater

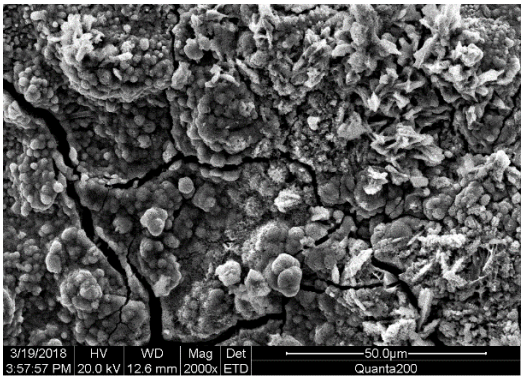

(a) 2 months rust layer morphology of A2 (x2000)

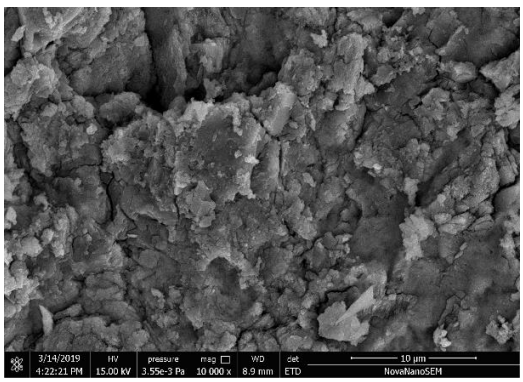

(b) 6 months rust layer morphology of A2 (x10000)

Fig.8 SEM images of rust layer of steel under dry-wet cycle

equations are as follows [9]:

$$Fe^{2+} + 8\gamma\text{–}FeOOH + 2e^{-} \rightarrow 3Fe_3O_4 + 4H_2O \quad (3)$$

$$3Fe_3O_4 + 3/4O_2 + 9/2H_2O \rightarrow 9\alpha\text{–}Fe_2O_3 \quad (4)$$

According to the results of XRD and SEM analyses, it can be speculated that goethite (α–FeOOH) and lepidocrocite (γ–FeOOH) dehydrate and transform into hematite (α–Fe_2O_3) after dehydration. Once the environment becomes damp, hematite (α–Fe_2O_3) can also absorb water and convert into goethite (α–FeOOH). γ–FeOOH can easily convert into more stable magnetite (Fe_3O_4). Magnetite (Fe_3O_4) can be reconverted to maghemite (γ–Fe_2O_3) and further oxidized to more stable goethite (α–FeOOH) by secondary changes under oxidation condition. With the diffusion of oxygen and water vapor, new lepidocrocite (γ–FeOOH) is constantly generated. Thus, the corrosion reaction constantly progresses, and the thickness of rust layer increases continuously.

4. CONCLUSIONS

In this paper, the compositions, the intrinsic morphology and the secondary electronic signal imaging of corrosion products of steel under different accelerated corrosion test methods and in different periods were analyzed by XRD and SEM. Based on the test results, the formation and development process of corrosion products of steel bars were discussed. The main conclusions are as follows:

(1) The passive film of reinforcing bar in concrete was destroyed mainly by electrochemical corrosion reaction. Under the action of oxygen and water, iron lost electrons and metal anodic dissolution occurred. The electrons obtained from oxygen and water resulted in the intermediate corrosion product $Fe(OH)_2$.

(2) Due to the presence of large amount of chloride ions, the internal rust layer contained a large number of transition products, including lepidocrocite (γ–FeOOH) and aka-ganeite (β–FeOOH).

(3) Under wet/dry cycling condition, steel corrosion products tended to form maghemite (γ–Fe_2O_3) and hematite (α–Fe_2O_3) due to dehydration, while hematite (α–Fe_2O_3) absorbed water and converted to goethite (α–FeOOH) with moisture. That is to say, with the supplement and loss of water in concrete, various corrosion products were dynamically transformed into each other.

(4) The content of lepidocrocite (γ–FeOOH) and aka-ganeite (β–FeOOH) observed in rusted steel samples immersed in the seawater for a long time was relatively small. The reason is that they can replace O_2 and H_2O to be depolarizers of cathodic reduction reaction without oxygen and consume themselves to ensure smooth corrosion.

REFERENCES

[1] Wu Q, Li X, Xu J, Wang G, Shi W, Wang S. Size Distribution Model and Development Characteristics of Corrosion Pits in Concrete under Two Curing Methods. Materials, Vol. 12, 2019, pp. 1846-1857.

[2] Yu C, Wu Q, Yang J. Effect of seawater for mixing on properties of potassium magnesium phosphate cement paste.Construction and Building Materials, Vol 155, Nov. 2017, pp. 217-227.

[3] Refait P, Génin J. The oxidation of ferrous hydroxide in chloride-containing aqueous media and Pourbaix diagrams of green rust one[J]. Corrosion Science, Vol 34, 1993, pp. 797-819.

[4] Legrand L, Sagon G, Lecomte S, et al. A Raman and infrared study of a new carbonate green rust obtained by electrochemical way. Corrosion Science, Vol. 43, 2001, pp. 1739-1749.

[5] Standard, A. S. T. M. (2013). D1141-98: Standard Practice for the Preparation of Substitute Ocean Water. ASTM International, West Conshohocken.

[6] Misawa T, Asami K, Hashimoto K, et al. The mechanism of atmospheric rusting and the protective amorphous rust on low alloy steel[J]. Corrosion Science, Vol. 14, 1974, pp. 279-289.

[7] Armstrong R D, Johnson B W, Wright J D. An investigation into the cathodic delamination of epoxy-polyamine protective coatings[J]. Electrochimica Acta, Vol. 36, 1991, pp. 1915-1923.

[8] Ji Y, Shen J, Wang L, et al. Experimental study on non-oxygen diffusion control of steel bar corrosion in concrete [J]. Journal of Hunan University, Natural Science Edition, Vol. 39, 2012, pp. 11-16.

[9] JI Y, ZHANG L, MA H, et al. Analysis on rusts of steel bar in concrete exposed to chloride-containing environment[J]. Journal of Central South University, Science and Technology, Vol. 11, 2012, pp. 49-55.